Molecular Biology of the Cell
Vol. 20, 4751–4765, November 15, 2009

Expression and Activity of Phosphodiesterase Isoforms during Epithelial Mesenchymal Transition: The Role of Phosphodiesterase 4

Ewa Kolosionek,* Rajkumar Savai,† Hossein Ardeschir Ghofrani,* Norbert Weissmann,* Andreas Guenther,* Friedrich Grimminger,*† Werner Seeger,*‡ Gamal Andre Banat,† Ralph Theo Schermuly,*‡ and Soni Savai Pullamsetti*‡

†Department of Hematology and Oncology, *University of Giessen Lung Centre, Giessen, Germany; and ‡Max-Planck-Institute for Heart and Lung Research, Bad Nauheim, Germany

Submitted January 7, 2009; Revised August 10, 2009; Accepted September 10, 2009
Monitoring Editor: Keith E. Mostov

Epithelial–mesenchymal transition (EMT) has emerged as a critical event in the pathogenesis of organ fibrosis and cancer and is typically induced by the multifunctional cytokine transforming growth factor (TGF)-β1. The present study was undertaken to evaluate the potential role of phosphodiesterases (PDEs) in TGF-β1-induced EMT in the human alveolar epithelial type II cell line A549. Stimulation of A549 with TGF-β1 induced EMT by morphological alterations and by expression changes of the epithelial phenotype markers E-cadherin, cytokeratin-18, zona occludens-1, and the mesenchymal phenotype markers, collagen I, fibronectin, and α-smooth muscle actin. Interestingly, TGF-β1 stimulation caused twofold increase in total cAMP-PDE activity, contributed mostly by PDE4. Furthermore, mRNA and protein expression demonstrated up-regulation of PDE4A and PDE4D isoforms in TGF-β1-stimulated cells. Most importantly, treatment of TGF-β1 stimulated epithelial cells with the PDE4-selective inhibitor rolipram or PDE4 small interfering RNA potently inhibited EMT changes in a Smad-independent manner by decreasing reactive oxygen species, p38, and extracellular signal-regulated kinase phosphorylation. In contrast, the ectopic overexpression of PDE4A and/or PDE4D resulted in a significant loss of epithelial marker E-cadherin but did not result in changes of mesenchymal markers. In addition, Rho kinase signaling activated by TGF-β1 during EMT demonstrated to be a positive regulator of PDE4. Collectively, the findings presented herein suggest that TGF-β1 mediated up-regulation of PDE4 promotes EMT in alveolar epithelial cells. Thus, targeting PDE4 isoforms may be a novel approach to attenuate EMT-associated lung diseases such as pulmonary fibrosis and lung cancer.

INTRODUCTION

Epithelial–mesenchymal transition (EMT), in which fully differentiated epithelial cells undergo transition to a mesenchymal phenotype giving rise to fibroblasts and myofibroblasts, is increasingly recognized as important not only in development but also in wound healing, fibrosis, and the invasion and metastasis of tumor cells (Greenburg and Hay, 1982; Thiery, 2002; Nawshad *et al*., 2005). The phenotypic conversion involves loss of epithelial polarity, loss of epithelial markers, cytoskeletal reorganization, and transition to a spindle-shaped morphology concomitant with acquisition of mesenchymal markers and an invasive phenotype (Kalluri and Neilson, 2003; Zavadil and Bottinger, 2005).

EMT, depending on the precise physiological context, can be induced either by environmental stresses/factors such as hypoxia (Higgins *et al*., 2007) and reactive oxygen species (ROS) (Rhyu *et al*., 2005) or by extracellular mediators, including TGF-β1, fibroblast growth factor-2, epidermal growth factor, connective tissue growth factor, insulin- like growth factor-2, interleukin-1, hepatocyte growth factor, and Wnt ligands (Moustakas and Heldin, 2007; Willis and Borok, 2007). Among these, TGF-β1, a multifunctional cytokine, has been shown to mediate EMT in vitro in several different cell lines, including alveolar epithelial cells (Miettinen *et al*., 1994; Kasai *et al*., 2005; Willis *et al*., 2005). Recently, in vivo evidence for TGF-β1–mediated EMT has been reported, confirming the master regulation role of TGF-β1 (Kim *et al*., 2006; Rees *et al*., 2006). Moreover, ROS have been shown to mediate TGF-β1–induced cellular responses in various cells, including EMT (Jiang *et al*., 2003; Brown *et al*., 2007), and it has been demonstrated that antioxidants effectively inhibited TGF-β1–induced EMT primarily through activation of mitogen-activated protein kinase (MAPK) and subsequently through extracellular signal-regulated kinase-directed activation of Smad in proximal tubular epithelial cells (Rhyu *et al*., 2005).

Cyclic nucleotide phosphodiesterases (PDEs) comprise a family of related proteins, which can be subdivided into 11 families (PDE1-PDE11) based on their amino acid sequences; sensitivity to different activators and inhibitors; and their

This article was published online ahead of print in *MBC in Press* (http://www.molbiolcell.org/cgi/doi/10.1091/mbc.E09–01–0019) on September 16, 2009.

Address correspondence to: Ralph Theo Schermuly (ralph.schermuly@mpi-bn.mpg.de).

Abbreviations used: Epithelial-to-Mesenchymal Transition (EMT); Transforming Growth Factor-β1 (TGF-β1); Phosphodiesterases (PDE); Reactive Oxygen Species (ROS).

ability to preferentially hydrolyze either cAMP, cGMP, or both. cAMP and cGMP are ubiquitous second messengers; consequently, PDEs propagate many signaling pathways, including proliferation, migration, and differentiation (Conti and Beavo, 2007).

Similarly, we postulated that PDE induction could play a role in regulating EMT. This hypothesis is based on earlier results that showed changes in cyclic nucleotides and PDEs can affect various differentiation processes. For example, remodeling of PDE isoforms was shown to influence monocyte-to-macrophage differentiation, myogenic differentiation, and fibroblast-to-myofibroblast conversion (Naro *et al*., 1999; Bender *et al*., 2005; Dunkern *et al*., 2007). Likewise, EMT in cultured Madin-Darby canine kidney cells were potentially inhibited by treatments that increase either cAMP or cGMP, such as PGD2 and PGE2 (Zhang *et al*., 2006) and nitric oxide in alveolar epithelial cells (Vyas-Read *et al*., 2007). Furthermore, epithelial and mesenchymal phenotype marker genes that are altered during EMT by TGF-β1 can be influenced by increased cAMP or cGMP levels (Santibanez *et al*., 2003; Liu *et al*., 2006). Finally, the attenuation of PDE has been shown to influence pathological processes by means of specific inhibitors that have demonstrated preclinical and clinical efficacy in the treatment of different lung diseases (Ghofrani *et al*., 2002; Huang and Mancini, 2006; Schermuly *et al*., 2007). In addition, the PDE4 inhibitor rolipram was shown to inhibit TGF-β1–stimulated ROS generation in mesangial cells for the induction of monocyte chemoattractant protein-1 expression (Cheng *et al*., 2005). However, until now the direct involvement of PDE family members and therapeutic value of PDE-specific inhibitors in the process of EMT has not been reported.

To address this question, we 1) ascertained the expression pattern of PDE isoforms upon TGF-β1–induced EMT of A549 cells via real-time reverse transcription-polymerase chain reaction (RT-PCR), PDE activity assays, and immunodetection experiments; 2) investigated whether altered PDE expression has a functional effect on cAMP accumulation and differentiation of A549 cells by using PDE isoform-specific inhibitors, PDE-specific small interfering RNAs (siRNAs), and PDE overexpression; and 3) elucidated the signaling pathways in the PDE-mediated regulation of EMT.

MATERIALS AND METHODS

Materials

The A549 cell line was obtained from American Type Culture Collection (Manassas, VA). DMEM/F-12, Opti-MEM, fetal bovine serum (FBS), streptomycin/penicillin, vitamins, and nonessentials amino acids were obtained from Invitrogen (Karlsruhe, Germany). TGF-β1 was obtained from R&D Systems (Minneapolis, MN). Rolipram and desmin antibody were obtained from Sigma-Aldrich (Munich, Germany). 3-Isobutyl-1-methylxanthine (IBMX) and cycloheximide were obtained from Calbiochem (Darmstadt, Germany). Lipofectamine, dihydroethidium (DHE), and Alexa 488-conjugated antibody were obtained from Invitrogen. Rho kinase (ROCK) inhibitor Y-27632 was obtained from Merck (Darmstadt, Germany). Im Prom reverse transcriptase and *Taq* polymerase PCR kit were obtained from Promega (Mannheim, Germany). Radioimmunoprecipitation assay (RIPA) buffer, Smad4, ERK1/2, phosphorylated (p)-ERK1/2, and TGF-β receptor II antibodies were obtained from Santa Cruz Biotechnology (Heidelberg, Germany). Glyceraldehyde-3-phosphate dehydrogenase (GAPDH) antibody was obtained from Novus (Littleton, CO). E-Cadherin antibody was obtained from Upstate Biotechnology (Schwalbachs, Germany). Cytokeratin antibody was obtained from Dako Deutschland (Hamburg, Germany). RhoA, PDE4A, and PDE4D antibodies were obtained from Abcam (Cambridge, United Kingdom). Smad2/3, p-Smad2, p-Smad3, p38, p-p38, and ROCK antibodies was obtained from Cell Signaling (Beverly, MA). siRNA for PDE4A was obtained from Eurogentec (Seraing, Belgium). siRNA for PDE4D and RhoA were obtained from Ambion (Darmstadt, Germany). Enhanced chemiluminescence (ECL) detection kit was obtained from GE Healthcare (Piscataway, NJ).

Cell Line and Culture Conditions

A549 cells were grown on 10-cm^2 dishes in DMEM/F-12 supplemented with 10% fetal calf serum (FCS), 5% streptomycin/penicillin, 5% vitamins, and 5% nonessentials amino acids. Cells were cultured from the time of plating in medium alone, and medium 0.1% FCS supplemented with TGF-β1 (2 ng/ml) for 24 h. For experiments with Rolipram, cells were pretreated with different concentrations of rolipram (100 nM or 1 μM) for 12 h followed by TGF-β1 (2 ng/ml) stimulation for 24 h. For experiments with Y-27632, cells were pretreated with Y-27632 (10 μM) for 12 h followed by TGF-β1 (2 ng/ml) stimulation for 24 h. For experiments with cycloheximide (CHX), cells were pretreated with CHX (5 μM) for 3 h followed by TGF-β1 (2 ng/ml) stimulation for 24 h. The dosages of TGF-β1, rolipram, Y-27632, and CHX were chosen on the basis of previous studies.

RNA Isolation and Real-Time RT-PCR

Total RNA was extracted from the cells with TRIzol Reagent (Invitrogen) following the manufacturer's protocols. The yield of extracted RNA was determined with Nano Drop (PeqLab, Erlangen, Germany). Two micrograms of total RNA was reverse-transcribed (RT) into cDNA using a Promega kit with oligo(dT)$_{18}$ primers according to the supplier's instructions. Real-time PCR (Stratagene QPCR using Invitrogen Mastermix SYBR kit) was performed using 1 μg of cDNA and 0.05 M forward/reverse primers; two primer sets were designed for each PDE isoform as described previously (Murray *et al*., 2007) as well as for epithelial and mesenchymal phenotype markers and RhoA (Table 1). Cycle conditions were 95°C for 10 min (1 cycle), 95°C for 30 s, 58°C for 30 s, and 72°C for 30 s (40 cycles). By using the MxPro QPCR software (Stratagene, Waldbronn, Germany), a dissociation curve was generated for each gene to ensure a single-product amplification, and the threshold cycle (Ct values) for each gene was determined. The comparative $2-\Delta\Delta$Ct method was used to analysis mRNA -fold changes between control and treatment (TGF-β1 alone or different treatments followed by TGF-β1 stimulation), which calculated as ratio = $2-(\Delta$Ct control $-$ ΔCt treatment), where Ct is the cycle threshold and ΔCt (Ct target $-$ Ct reference) is the Ct value normalized to reference gene Porphobilinogen deaminase (PBGD) obtained for the same cDNA samples.

PDE Activity Assay

PDE activity assay was performed with a modification of the two-step method by Thompson and Appleman (1971). Cells were lysed in RIPA buffer containing dimethyl sulfoxide (DMSO), protease inhibitor cocktail, and phenylmethylsulfonyl fluoride (PMSF). Cells were subjected to a low-speed centrifugation (13,000 $\times$ *g* for 10 min), and aliquots of the resulting supernatant were assayed for PDE activity by using cAMP (1 μM) spiked with [^{3}H]cAMP as a substrate. All assays were carried out at 37°C for 15 min and then terminated by boiling for 3 min. *Crotalus atrox* venom was added to prevent resynthesis of cAMP, and the products of cAMP were separated from unhydrolyzed substrate on chromatography columns filled with Sephadex-Q25 beads (GE Healthcare). Total PDE activity in cell lysates was determined and is expressed as picomoles of cAMP hydrolyzed per minute per milligram of lysate protein. PDE activities were determined using IBMX for nonspecific PDE inhibition except for PDE9 (5 mM) and with specific inhibitor rolipram for PDE4 (1 μM).

Immunoblotting

Cells were lysed in RIPA buffer containing DMSO, protease inhibitors, and PMSF. To detect proteins, lysates were subjected to SDS-polyacrylamide gel electrophoresis, electrophoretically transferred to nitrocellulose membrane, blocked for 1 h in 5% nonfat milk, and probed with the appropriate primary antibody overnight at 4°C at the following dilutions: GAPDH (1:5000), E-cadherin (1:1000), cytokeratin-18 (1:1000), desmin (1:500), fibronectin (1:1000), PDE4A (1:1000), PDE4D (1:1000), Smad4 (1:500), Smad2/3 (1:500), p-Smad2 (1:500), p-Smad3 (1:500), TGF-β receptor II (1:1000), ROCK1 (1:1000), RhoA (1:1000), ERK (1:1000), p-ERK (1:1000), p38 (1:1000), and p-p38 (1:1000). Subsequently, the membranes were washed with wash buffer and incubated with the respective horseradish peroxidase-conjugated polyclonal secondary antibodies for 1 h at room temperature (RT). Antibody complexes were visualized by enhanced chemiluminescence using an ECL kit.

Immunofluorescence

Stimulated and nonstimulated A549 cells were grown on chamber slides. Slides were fixed with cold acetone-methanol (1:1) for 10 min at RT. After rinsing in phosphate-buffered saline (PBS) and blocking in 5% bovine serum albumin for 1 h in RT, cells were incubated overnight at 4°C with PBS containing PDE4A (1:100), PDE4D (1:100), E-cadherin (1:200), cytokeratin-18 (1:200), α-smooth muscle actin (α-SMA; 1:100), and fibronectin (1:100). Indirect immunofluorescence was conducted by incubation with Alexa 488-conjugated goat anti-rabbit immunoglobulin (Ig)G antibodies or Alexa 488-conjugated goat anti-mouse IgG antibodies. At the end of the procedure, fluorescence images were captured using the same exposure times and conditions with the fluorescence microscope (Leica Microsystems, Wetzlar, Germany). Fluorescein isothiocyanate (FITC) (filter I3, no. 513808) fluorescence images were captured for 690 ms, and 4,6-diamidino-2-phenylindole (DAPI) images for (filter A, no. 513804) 1.45 ms with a digital camera (DC 300 FX; Leica

Table 1. Forward and reverse primer sequences for epithelial and mesenchymal markers and for each PDE isoform investigated using real-time PCR

Gene	NM no.	Forward primer	Reverse primer
E-Cadherin	NM_004360	TGCCCAGAAAATGAAAAAGG	GTGTATGTGGCAATGCGTTC
Cytokeratin-18	NM_002276	CAAAGCCTGAGTCCTGTCCT	GAGATCCGGGAACCAGAG
Zona Occludens-1	NM_003257	CTTTAGGCTCCTGGATTTGG	AGGAACACTGCTTGTTGCAC
Collagen I	NM_000088	TGTTCAGCTTTGTGGACCTC	GCAAGGCGCGATATAGAGTA
Fibronectin	NM_002026	AGCCTCGAAGAGCAAGAGG	CAAAACTTCAGCCCCAACTT
α SMA	NM_001613	GAGAAGAGTTACGAGTTGCCTGA	TGTTAGCATAGAGGTCCTTCCTG
PDE1A	NM_001003683	AGGTCACTTCCAGCAAATTA	CCACATAGGAAGAAGTTTCG
PDE1B	NM_000924	GCTTTGATGTCTTTTCCTTG	ATTCTGACTTGGTCTGGATG
PDE1C	NM_005020	AGATATTAGCCATCCAGCAA	CAACGGAGATGACAGAAT
PDE2A	NM_002599	CCTTCAACAAGCTAGAAGGA	CGGATCTCATAGCTCTCATC
PDE3A	NM_000921	CAACACTGTGTGTGTGTGTG	CAAGTGGTGCATAGCAGTAA
PDE3B	NM_000922	GATGAAGAAGCAAATCTTGG	TTCTCCACCTGCAGTTTATT
PDE4A	NM_006202	GCTGAAGACCTCATCGTAAC	ATTCTGTTTGTCCAGGAATG
PDE4B	NM_002600	ATTCTGTTTGTCCAGGAATG	ATGCTGGTGTAGAAAGGAGA
PDE4C	NM_000923	AGAGTGGTACCAGAGCAAGA	TGGGAGCCACCTATAACTAA
PDE4D	NM_006203	CACCAAATGACCTTACCTGT	AGCTCCACTGTTACCTTTCA
PDE5A	NM_001083	GAAAAGGACTTTGCTGCTTA	TGATTTTGTTTGCATCATGT
PDE7A	NM_002603	GCAATATGAATTTGGCTTTC	GGAAAGAGCTGCAGTCTAAA
PDE7B	NM_018945	TCTTCAATACCCATGGACTC	ATCCTGTGTCATTTCCTTTG
PDE8A	NM_002605	ACCAATGTAATGGATTCTGC	TGAGTTACAAGCCCTGAGTT
PDE8B	NM_003719	AGAACAGGAGGAAAGAGTCC	CGTTTCCTGACAGTCTTCTC
PDE9A	NM_002606	TGTCCACGACAACTACAGAA	GTGGCCAAGATTAATGTGAT
PDE10A	NM_006661	AGCAGGTACCAAGATACGAA	TGATTCCAGTCCAGTACCTC
PDE11A	NM_016953	ATGCAGATCAACGACTTTTT	CCGATAGTTTTTCCTCACTG

Microsystems) attached to the microscope. Using Qwin V3 software (Leica Microsystems), FITC and DAPI images were merged and fluorescent intensity levels were quantified as described previously (Savai *et al*., 2005, 2007).

ROS Detection

Superoxide release from A549 was measured using the superoxide-sensitive dye DHE. In brief, the cells were grown on chamber slides and cultured in medium alone, 0.1% FBS medium supplemented with TGF-β1 (2 ng/ml), TGF-β1 (2 ng/ml) and rolipram (1 μM), TGF-β1 (2 ng/ml) and PDE4A, and/or PDE4D-specific siRNA (100 nM), TGF-β1 (2 ng/ml) and Smad3 inhibitor SIS3 (10 and 30 μM) or H_2O_2 (10 mM) for 24 h. H_2O_2 treatment served as the positive control. Subsequently, the cells were incubated with DHE (5 μM) for 30 min. The cells were washed with PBS, fixed in acetone and methanol (1:1) for 10 min, and stained with the nuclear stain DAPI. Cells were visualized under fluorescent microscopy (excitation, 514 nm; emission, 560 nm). In total, 10 images were captured from each group and in each image the total fluorescence-integrated density was analyzed from all groups, respectively, in a blinded manner using ImageJ software (National Institutes of Health, Bethesda, MD).

RNA Interference

siRNA oligonucleotides specific for PDE4 and RhoA (si1-PDE4A 5′-CCUGCAUCAUGUACAUGAUtt-3′, si2-PDE4A 5′-GAGUACAUUUCCACAACAUtt-3′, si3-PDE4A 5′-CAGCGACUAUGACAUGUCAtt-3′, sense PDE4D-5′-GAGUCGGUCUGGAAAUCACtt-3′; antisense PDE4D-5′-UUGAUUUCCAGACCGACUCat-3′), RhoA (sense RhoA-5′-CACAGUUGUUUGAGAACUAUtt-3′, antisense RhoA-5′-AUAGUUCUCAAACACUGUGgg-3′), and scramble siRNA (si-control) (dTdT 3′ overhang). Transient transfection of siRNA was performed with Lipofectamine according to the manufacturer's protocols. A549 cells were subcultured to 70% confluence in DMEM/F-12 medium supplemented with 10% FBS. Transfection of 100 nM siRNA was performed in Opti-MEM for 6 h, followed by culturing in DMEM/F-12 supplemented with 10% FBS up to 24 h (RNA isolation) or 48 h (protein isolation).

PDE4 Overexpression

All cloning was performed using the Gateway cloning system (Invitrogen, Carlsbad, CA). Human PDE4A and PDE4D were subcloned into the pDEST26 expression vector. Transient transfection of PDE4A and PDE4D vector constructs was performed with Lipofectamine (Invitrogen) according to the manufacturer's protocols. A549 cells were subcultured to 70% confluence in DMEM/F-12 supplemented with 10% FBS. Transfection of 2 μg of constructs was performed in Opti-MEM for 6 h, followed by culturing in DMEM/F-12 supplemented with 10% FBS up to 24 h (RNA isolation) or 48 h (protein isolation).

Statistical Analysis

Data are expressed as the mean ± SEM. Statistical comparisons between two populations were performed using paired and unpaired Student's *t* tests where appropriate or by one-way analysis of variance in combination with a Student–Newman–Keuls post hoc test, which was used to compare differences between multiple groups, with a probability value of $p < 0.05$ considered to be significant.

RESULTS

Effects of TGF-β1 on Cell Morphology and the Expression of Phenotype Markers in A549 Cells

As shown in Figure 1A, A549 cells in the absence of TGF-β1 exhibited a cubic, epithelioid shape and cluster formation, the typical features of epithelial cells. On TGF-β1 stimulation for 24 h, phase contrast microscopy revealed that the cells underwent a morphological change, from cobblestone-like cell morphology to an elongated and spindle-like morphology, and reduced their cell–cell contact.

Furthermore, the mRNA expression of epithelial phenotype markers E-cadherin, cytokeratin-18, and zona occludens-1 was significantly altered in TGF-β1–stimulated cells compared with control cells. TGF-β1 stimulation significantly decreased E-cadherin expression in a concentration-dependent manner. Concentrations as low as 1 ng/ml TGF-β1 induced significant down-regulation of E-cadherin, cytokeratin-18, and zona occludens-1 expression (Figure 1B). Furthermore, immunoblotting confirmed decreased protein expression of both E-cadherin and cytokeratin-18 in TGF-β1–stimulated cells (Figure 1, C and D).

In parallel with the marked decrease in the epithelial phenotype markers, TGF-β1 significantly induced mRNA expression of the mesenchymal markers collagen I, fibronectin, and α-SMA in a concentration-dependent manner (Figure 1E). However, the extent of α-SMA expression at low concentrations of TGF-β1 was not as profound as fibronectin and colla-

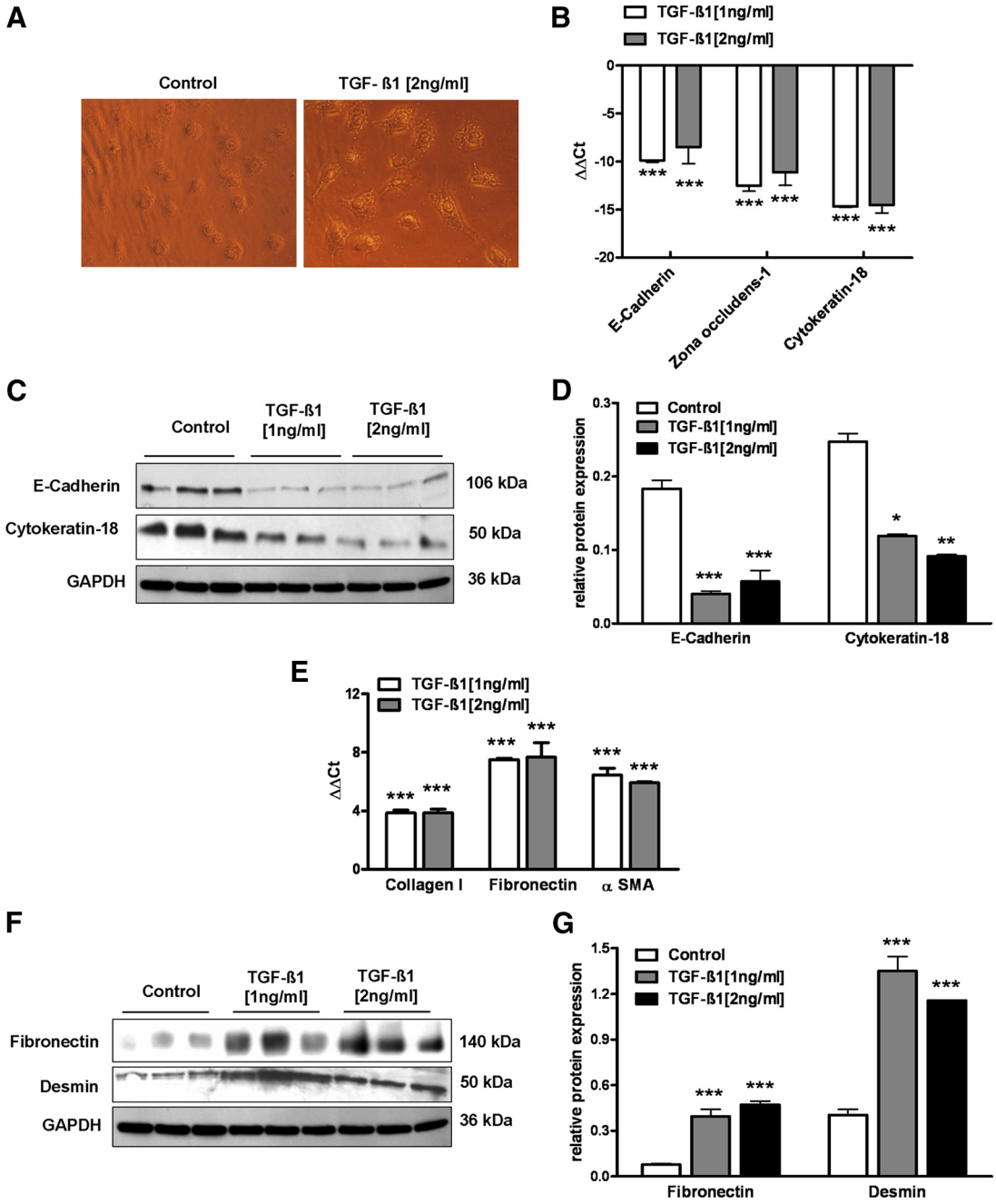

Figure 1. Effect of TGF-β1 stimulation on cell morphology and epithelial phenotype marker expression. (A) A549 cells were stimulated with TGF-β1 (2 ng/ml) for 24 h. Cell morphology was examined using phase contrast microscopy. (B) mRNA expression as analyzed by real-time RT-PCR of the epithelial phenotype markers E-cadherin, zona occludens-1, and cytokeratin-18 in TGF-β1 (1 and 2 ng/ml)-stimulated (24 h) and control cells. (C) Protein expression as analyzed by immunoblotting. (D) Subsequent densitometric quantification of epithelial phenotype markers (E-cadherin and cytokeratin-18) in TGF-β1 (1 and 2 ng/ml)-stimulated (24 h) and control cells are indicated. (E) mRNA expression as analyzed by real-time RT-PCR of mesenchymal phenotype markers, collagen I, fibronectin, and α-SMA in TGF-β1 (1 and 2 ng/ml)-stimulated (24 h) and control cells. (F) Protein expression as analyzed by immunoblotting. (G) Subsequent densitometric quantification of mesenchymal phenotype markers (fibronectin and desmin) in TGF-β1 (1 and 2 ng/ml)-stimulated (24 h) and control cells. All values are given as the mean ± SEM (n = 4) and are normalized to PBGD (B and E) or GAPDH (D and G). *$p < 0.05$, **$p < 0.01$, and ***$p < 0.001$ versus control.

gen I. Similarly, immunoblotting demonstrated increased immunoreactivity of fibronectin and desmin in TGF-β1–treated cells compared with control cells (Figure 1, F and G).

PDE Expression and Activity during TGF-β1–induced EMT

Real-time RT-PCR demonstrated an increase in mRNA expression of three PDE isoforms in TGF-β1–stimulated cells compared with control: PDE4A, PDE4D, and PDE8A, with PDE4D showing the most prominent increase in mRNA. In contrast, PDE1A, PDE3A, and PDE7B expressions were decreased by TGF-β1 stimulation (Figure 2, A and B). Moreover, time course of PDE4 induction revealed that PDE4A as well as PDE4D level was increased by TGF-β1 as early as 6 h after stimulation (Figure 2C), whereas immunoblot-

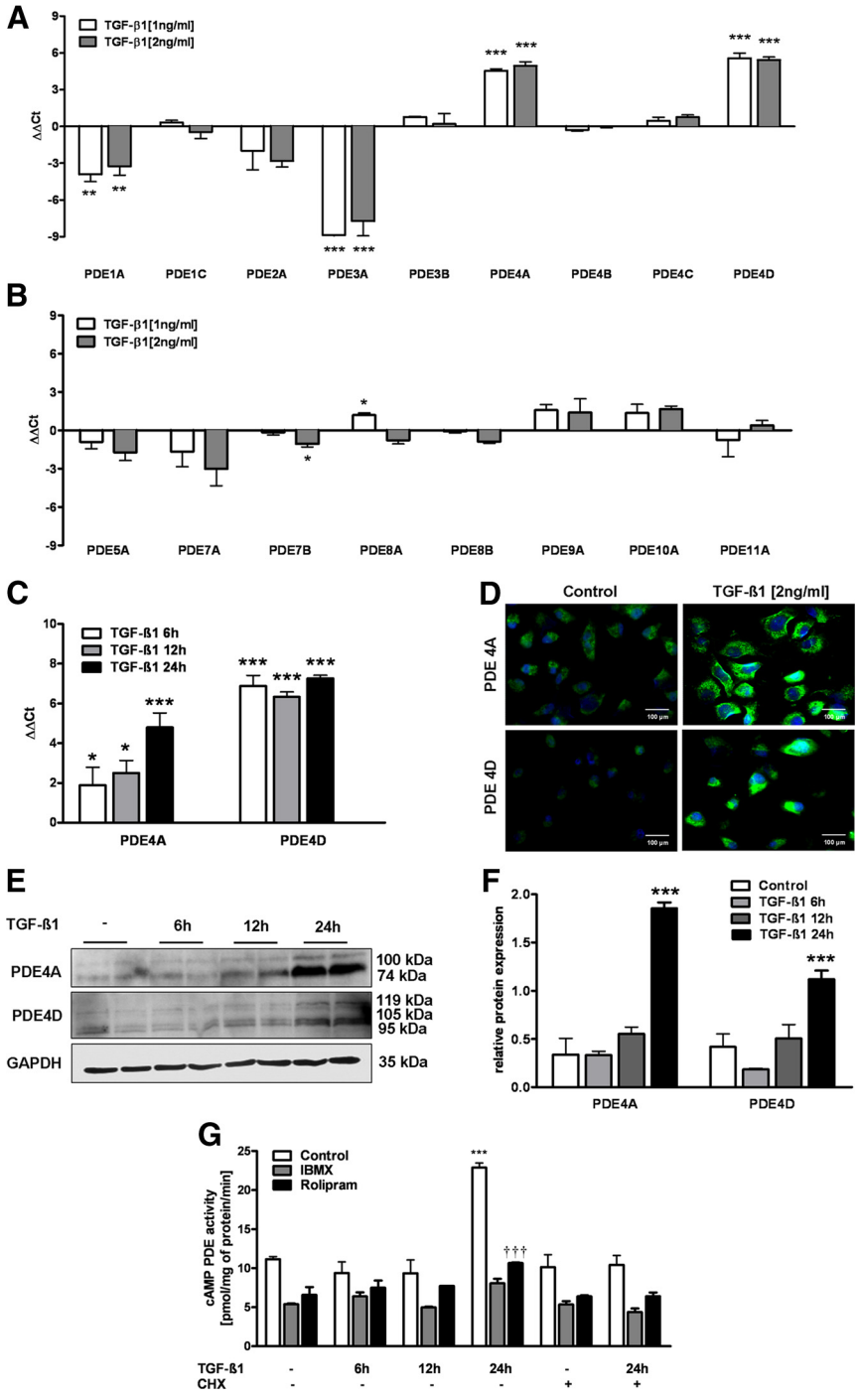

Figure 2. Expression, localization and activity of multiple PDE isoforms during TGF-β1–induced EMT. (A and B) mRNA expression of multiple PDE isoforms were analyzed by real-time RT-PCR in TGF-β1 (1 and 2 ng/ml)-stimulated (24 h) and control cells. (C) mRNA expression of PDE4 isoforms (PDE4A and PDE4D) were analyzed by real-time RT-PCR in TGF-β1–stimulated (6, 12, and 24 h) and control cells. (D) Localization of PDE4 isoforms (PDE4A and PDE4D) in TGF-β1 (2 ng/ml)–stimulated (24 h) and control cells, as analyzed by immunofluorescence. (E) Protein expression as analyzed by immunoblotting. (F) Subsequent densitometric quantification of PDE4 isoforms (PDE4A and PDE4D) in TGF-β1 (1 and 2 ng/ml)–stimulated (6, 12, and 24 h) and control cells. (G) cAMP-PDE activity of A549 cells treated with TGF-β1 (2 ng/ml) (6, 12, and 24 h) and after using CHX as analyzed by PDE activity assay using cAMP-PDE inhibitors [30 μM 8-MM-IBMX, and PDE4, 1 μM rolipram]. The relative contribution of each isoform to the total cAMP PDE activity was calculated. All values are given as the mean ± SEM (n = 4) and are normalized to PBGD (A–C) or GAPDH (F). *$p < 0.05$, **$p < 0.01$, and ***$p < 0.001$ versus control.

ting demonstrated up-regulation of both PDE4A isoforms (PDE4A1 74 kDa and PDE4Ax 100 kDa) and PDE4D isoforms (PDE4D3 95 kDa, PDE4D4 105 kDa, and PDE4D5 119 kDa) after 24-h stimulation (Figure 2, E and F). Furthermore, immunofluorescence displayed PDE4A- and PDE4D-like immunoreactivity in the cytoplasm. PDE4A was variably found to be diffusely present in the membrane of the A549 cells (Figure 2D).

Interestingly, total cAMP-PDE activity was increased twofold in TGF-β1–stimulated cells compared with control (Figure 2G). Using cAMP-PDE inhibitors (30 μM 8-MM-IBMX and PDE4, 1 μM rolipram), we calculated the relative contribution to the total cAMP PDE activity and found PDE4 to be the major contributor to cAMP-PDE activity. Furthermore, to determine whether TGF-β1 regulates posttranslationally PDE4 enzymatic activity, TGF-β1–stimulated A549 cells at different time points were treated with CHX followed by assessment of cAMP-PDE activity. As indicated in Figure 2G, after protein synthesis inhibition by CHX treatment, the endogenous cAMP-PDE activity as well as PDE4 activity levels in both TGF-β1–stimulated and nonstimulated cells remained unaltered, indicating that TGF-β1 has no influence on posttranslationally PDE4 enzymatic activity (Figure 2G).

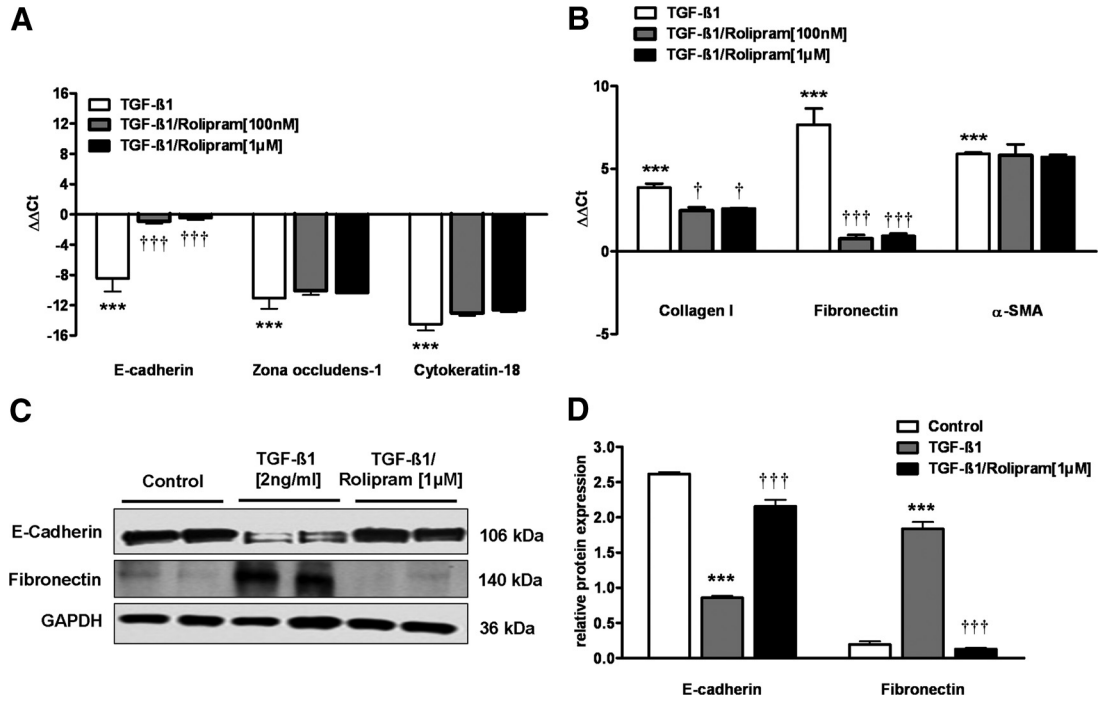

Figure 3. Effect of PDE4 inhibition on epithelial and mesenchymal phenotype markers expression in TGF-β1–induced EMT. A549 cells were pretreated with PDE4 inhibitor rolipram (100 nM or 1 μM) for 12 h followed by TGF-β1 (2 ng/ml) stimulation for 24 h or stimulated with TGF-β1 (2 ng/ml) alone. (A) mRNA expression as analyzed by real-time RT-PCR of epithelial phenotype markers (E-cadherin, zona occludens-1, and cytokeratin-18). (B) mRNA expression as analyzed by real-time RT-PCR of mesenchymal phenotype markers (collagen I, fibronectin, and α-SMA) in the above-mentioned treated cells. (C) Protein expression as analyzed by immunoblotting. (D) Subsequent densitometric quantification of epithelial and mesenchymal phenotype marker (E-cadherin and fibronectin) in the above-mentioned treated cells. All values are given as the mean ± SEM (n = 4) and are normalized to PBGD (A and B) or GAPDH (D). *$p < 0.05$, **$p < 0.01$, and ***$p < 0.001$ versus control; †$p < 0.05$, ††$p < 0.01$, and ††† $p < 0.001$ versus TGF-β1–stimulated cells.

Effect of PDE4 Inhibition and siRNA-mediated Knockdown on TGF-β1–induced EMT

On the basis of the prominent increase in the mRNA and protein expression of PDE4A and PDE4D during TGF-β1–induced EMT, we assessed the role of the PDE4 family by using the specific pharmacological inhibitor rolipram. Figure 3 and 4 show changes in both epithelial and mesenchymal phenotype markers (mRNA and protein) in TGF-β1–stimulated A549 cells after treatment with rolipram. Rolipram (100 nM and 1 μM) significantly restored the mRNA expression of epithelial marker E-cadherin (Figure 3A). Incubation of the cells with rolipram (1 μM) also helped to abolish mRNA expression of the mesenchymal markers fibronectin and collagen I but not α-SMA (Figure 3B). Similarly, immunoblotting suggested down-regulation of E-cadherin (1.5-fold) and up-regulation of fibronectin (1.7-fold) with TGF-β1 stimulation. Treatment with rolipram restored E-cadherin and decreased fibronectin expression to nearly control level compared with TGF-β1–stimulated cells (Figure 3, C and D), demonstrating that PDE4 inhibition potentially abrogates TGF-β1 induced EMT.

Immunofluorescence analysis showed that E-cadherin staining was intense and restricted to cell–cell contacts in control cells and a complete disappearance of E-cadherin at cell–cell contacts was observed in TGF-β1–stimulated cells. However, the intensity of E-cadherin staining and membrane localization is restored in rolipram-treated cells (Figure 4, A and B). Similarly, staining intensity of cytokeratin-18 that exhibits a filament pattern throughout the cytoplasm is decreased in TGF-β1–stimulated cells that were partially preserved by rolipram treatment (Figure 4, A and C). In contrast, increased staining of fibronectin and α-SMA in cytoskeleton filaments was observed in TGF-β1–stimulated cells. Fibronectin expression is significantly abolished in rolipram-treated cells, although no changes in total α-SMA levels were detected (Figure 4, A, C, and D).

To be more specific with PDE4 inhibition, siRNA targeting PDE4A and PDE4D were applied to knock down endogenous PDE4A and PDE4D. As shown on Figure 5, PDE4A and PDE4D siRNAs each successfully knockdown the expression of corresponding endogenous mRNAs (Figure 5A). Down-regulation of PDE4A, PDE4D protein expression was also confirmed by immunoblotting (Figure 5, B and C). Furthermore, to determine the effects on TGF-β1–induced EMT, PDE4A, PDE4D, or both PDE4A and PDE4D siRNAs were transfected into A549 cells, followed by stimulation of the cells with TGF-β1. In cells transfected with either PDE4A siRNA or PDE4D siRNA alone, knock down abolished TGF-β1–induced E-cadherin repression and fibronectin induction at the mRNA level (Figure 6, A–D) as well as at the protein level (Figure 6E–H). Interestingly, transfection of both PDE4A and PDE4D siRNAs showed no additive effects on those markers compared with PDE4A or PDE4D siRNAs alone. Control siRNA showed no influences on those markers (Figure 6).

Effect of PDE4 Inhibition on TGF-β1–induced Smad Signaling

Because Smad proteins mediate many of the signaling responses induced by TGF-β1, we sought to determine whether PDE inhibition attenuates TGF-β1–induced EMT through regulation of Smad signaling pathway. As shown in

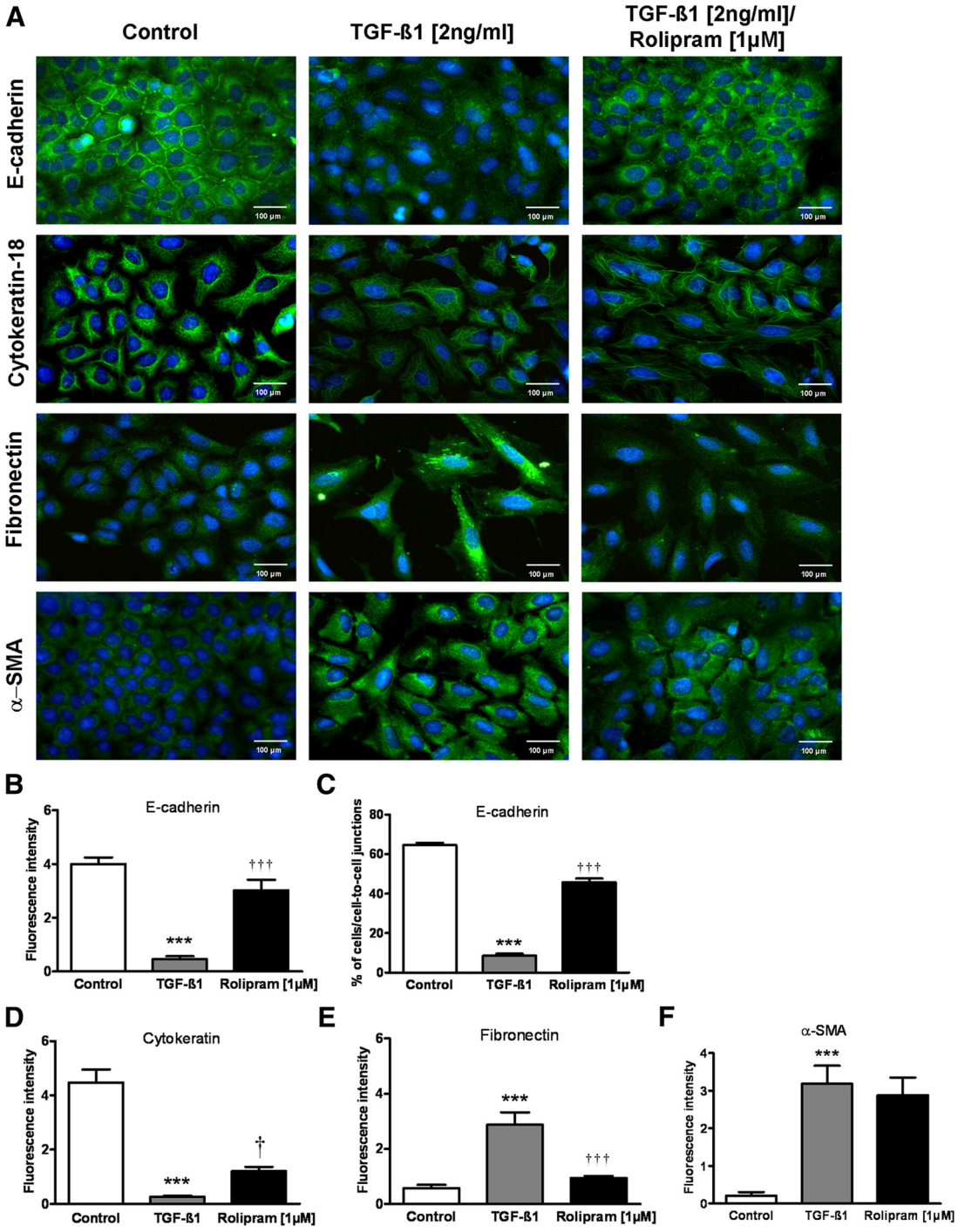

Figure 4. Effect of PDE4 inhibition on epithelial and mesenchymal phenotype markers localization in TGF-β1–induced EMT. A549 cells were pretreated with PDE4 inhibitor rolipram (1 μM) for 12 h followed by TGF-β1 (2 ng/ml) stimulation for 24 h or stimulated with TGF-β1 (2 ng/ml) alone. (A) Fluorescence images showed the localization of epithelial (E-cadherin and cytokeratin-18) and mesenchymal (fibronectin and α-SMA) phenotype markers. Bar, 100 μm. (B–E) Fluorescence intensity of E-cadherin; quantification of cells featuring E-cadherin at cel–cell contact; and fluorescence intensity of cytokeratin-18, fibronectin, and α-SMA were measured, respectively. All values are given as the mean ± SEM (n = 4). *$p < 0.05$, **$p < 0.01$, and ***$p < 0.001$ versus control; †$p < 0.05$, ††$p < 0.01$, †††$p < 0.001$ versus TGF-β1–stimulated cells.

Figure 7, the effects of rolipram on Smad signaling pathway was studied by immunoblotting with Smad4, Smad2/3, phospho-Smad2 (p-Smad2), phospho-Smad3 (p-Smad3), and TGF-β1 type II receptor (RII) antibodies. Phosphorylation of Smad2 and Smad3 proteins increased in A549 cells upon TGF-β1 stimulation for 24 h; however, these increases were not blocked by treatment with rolipram (Figure 7, A and B). Likewise, Smad4 and TGF-β1 RII protein levels increased after TGF-β1 stimulation, and this increase was not blocked by rolipram (Figure 7, A and B), indicating that PDE4 inhibitors did not inhibit TGF-β1–induced EMT through Smad phosphorylation.

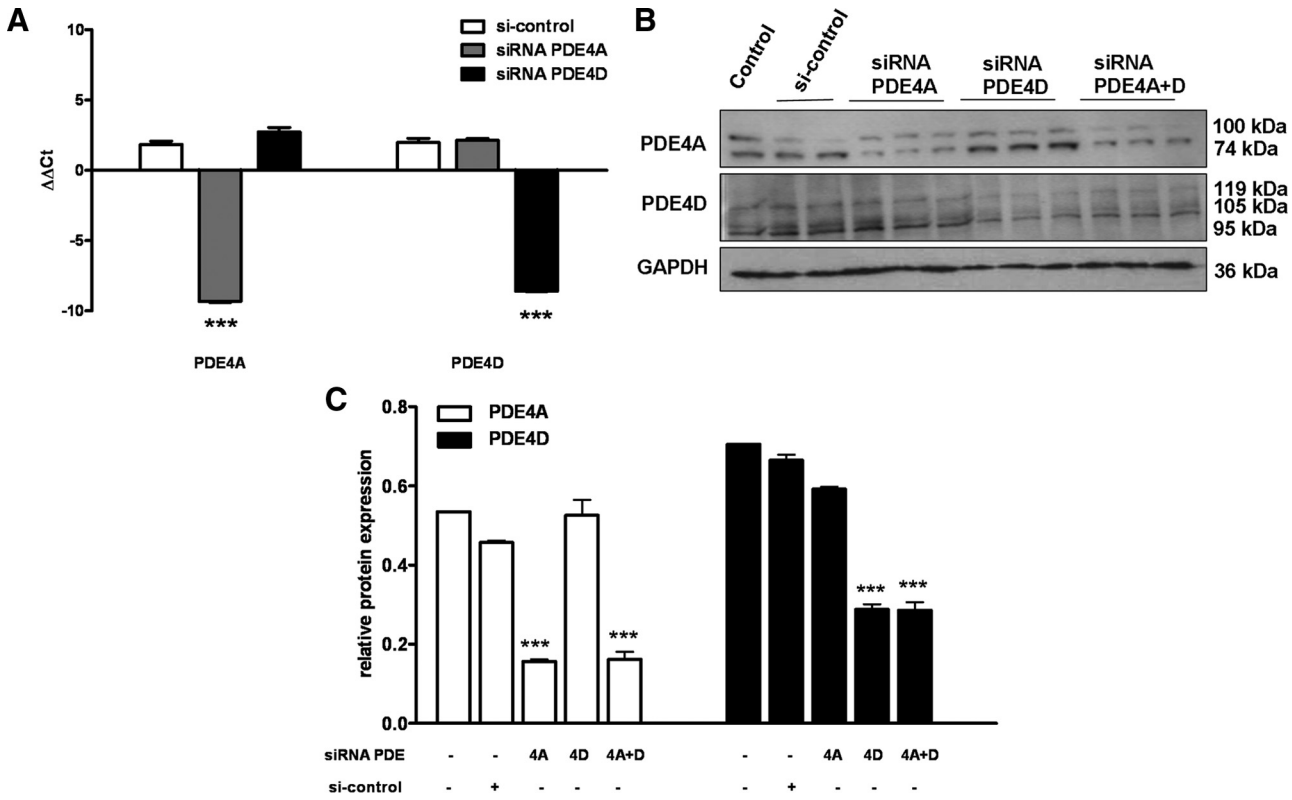

Figure 5. siRNA-mediated knockdown of PDE4A and PDE4D. A549 cells were transiently transfected with 100 nM control siRNA (si-control) or 100 nM PDE4A siRNA, PDE4D siRNA, or both (PDE4A+PDE4D) siRNAs for 24 h (mRNA expression) or 48 h (protein expression). (A) mRNA expression of PDE4A and PDE4D as analyzed by real-time RT-PCR. (B) Protein expression as analyzed by immunoblotting. (C) Subsequent densitometric quantification of PDE4A and PDE4D in the above-mentioned treated cells. All values are given as the mean ± SEM (n = 4) and are normalized to PBGD (A) or GAPDH (C). *$p < 0.05$, **$p < 0.01$, and ***$p < 0.001$ versus control.

Effect of PDE4 Inhibition and Knockdown on TGF-β1–induced ROS Production

In addition to the Smad pathway, TGF-β1 may signal through other pathways such as ROS, RhoA, and MAPK, we sought to determine the effects of PDE4 inhibition on these signaling cascades. To assess the role of ROS, DHE immunofluorescence was performed on cells treated with H_2O_2, TGF-β1 alone, TGF-β1 and/or rolipram for 24 h, TGF-β1 and knockdown of PDE4A and/or PDE4D. As shown in Figure 8A, H_2O_2 (10 mM) used as a positive control increased ROS production compared with control. Similarly, TGF-β1 (2 ng/ml) treatment increased ROS production. Inhibiting Smad pathway by using Smad3 inhibitor SIS3 (10 and 30 μM), significantly reduced ROS generation in concentration-dependent manner. Interestingly, TGF-β1 treatment induced ROS production, whereas cotreatment with rolipram or PDE4A and/or PDE4D blocked the TGF-β1–mediated increase in ROS production.

Next, we assessed the effects on TGF-β1–induced activation of ERK1/2 and p38, which are both involved in EMT. Phosphorylation of ERK and p38 increased in A549 cells upon TGF-β1 stimulation for 24 h. This increased phosphorylation is potently suppressed by siRNAs targeting PDE4A, PDE4D, or both PDE4A and PDE4D (Figure 8, B and C).

Effect of ROCK Inhibition and RhoA Knockdown on TGF-β1–induced PDE4 Expression

Our results indicated that TGF-β1 stimulation increased the expression of ROCK1 in A549 cells after 6 h of stimulation (Figure 9, A and B); therefore, involvement of RhoA/ROCK signaling pathway was assessed by using a specific pharmacological inhibitor of ROCK, Y-27632, and RhoA-specific siRNA. Treatment with Y-27632 partially abrogated TGF-β1–induced EMT and restored the expression of E-cadherin. Most importantly, PDE4A and PDE4D protein levels increased after TGF-β1 stimulation were decreased by Y-27632 treatment (10 μM) (Figure 9, C and D).

To be more specific with Rho kinase pathway inhibition, specific siRNA targeting RhoA was applied. Figure 9, E–G, shows RhoA expression was successfully suppressed by RhoA siRNA on mRNA and protein level, whereas RhoA expression did not change by control siRNA. With established siRNA conditions, PDE4A and PDE4D expression were examined. TGF-β1 induced up-regulation of PDE4A and PDE4D at the mRNA level was potently suppressed by RhoA siRNA (Figure 9H). However, immunoblotting revealed that only PDE4A, but not PDE4D expression was decreased by RhoA siRNA (Figure 9, I and J).

Effects of PDE4 Overexpression on the Expression of Phenotype Markers in A549 Cells

To unveil the possible role of PDE4 in the induction of EMT independent of TGF-β1 in A549 cells, A549 cells were transiently transfected with PDE4A, PDE4D, or both PDE4A and PDE4D expression plasmid or empty vector. Real-time RT-PCR indicated that PDE4A or PDE4D mRNA was dramatically increased in PDE4 constructs transfected cells compared with empty vector transfected cells (Figure 10A).

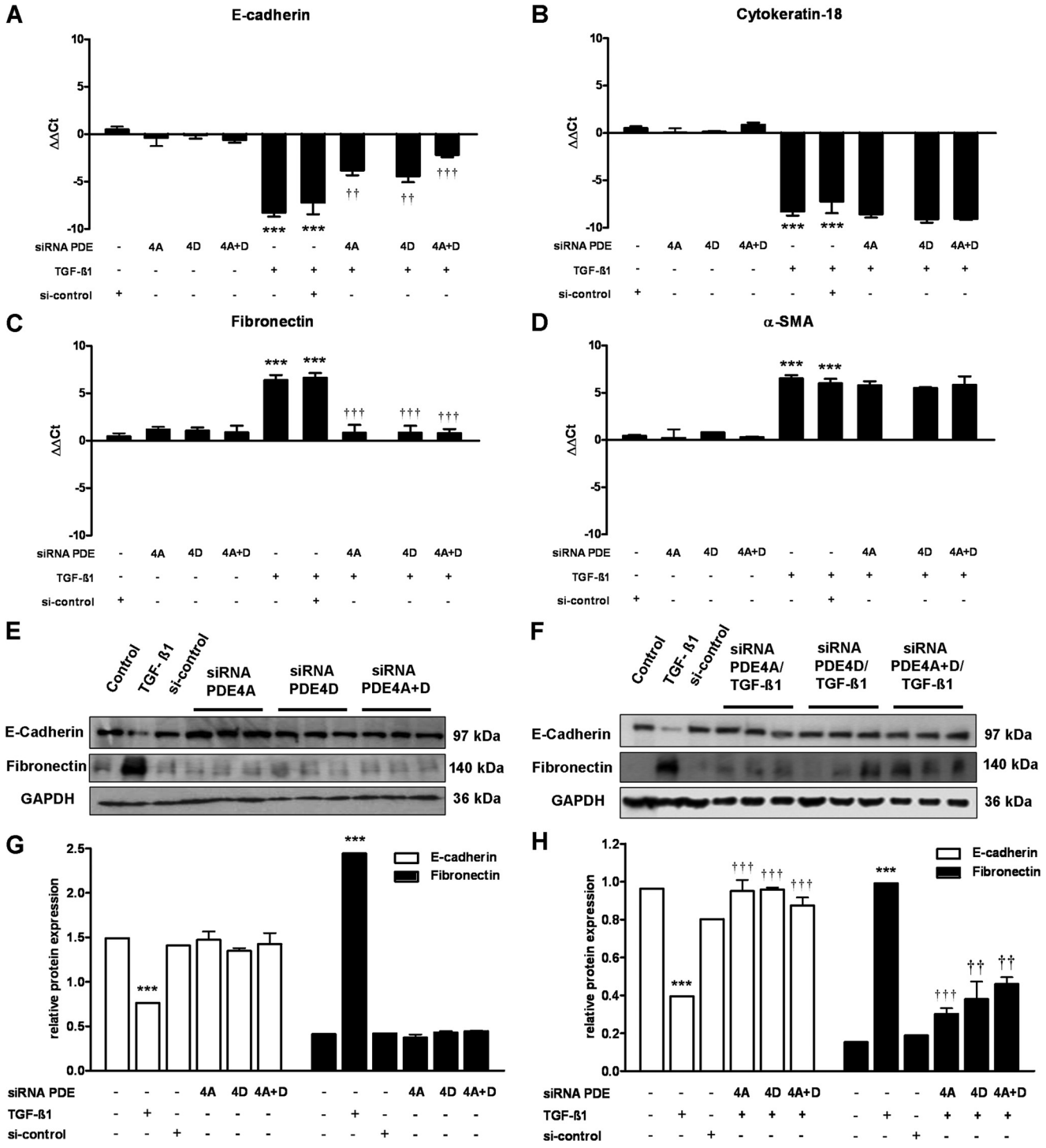

Figure 6. Effect of PDE4A and/or PDE4D knockdown by specific siRNA on TGF-β1–induced EMT. A549 cells were transiently transfected with 100 nM control siRNA (si-control) or 100 nM PDE4A siRNA, PDE4D siRNA, or both (PDE4A+PDE4D) siRNAs for 24 h (mRNA expression) or 48 h (protein expression) followed by without or with TGF-β1 (2 ng/ml) stimulation. mRNA expression of E-cadherin (A), cytokeratin-18 (B), fibronectin (C), and α-SMA (D) as analyzed by real-time RT-PCR. (E and F) Protein expression as analyzed by immunoblotting. (G and H) Subsequent densitometric quantification of E-cadherin and fibronectin in cells treated without or with TGF-β1, respectively. All values are given as the mean ± SEM (n = 4) and are normalized to PBGD (A–D) or GAPDH (G and H). *$p < 0.05$, **$p < 0.01$, and ***$p < 0.001$ versus control; †$p < 0.05$; ††$p < 0.01$, and †††$p < 0.001$ versus TGF-β1–stimulated cells.

Moreover, we observed an expression of His tag protein in these cells with no change in the expression of GAPDH protein (Figure 10B). To further assess whether PDE4 alone was able to induce EMT independent of TGF-β1 stimulation in A549 cells, we determined the expression of epithelial and mesenchymal markers. Interestingly, the transient expression of PDE4A and/or PDE4D resulted in a significant loss of epithelial marker E-cadherin at the mRNA and at the

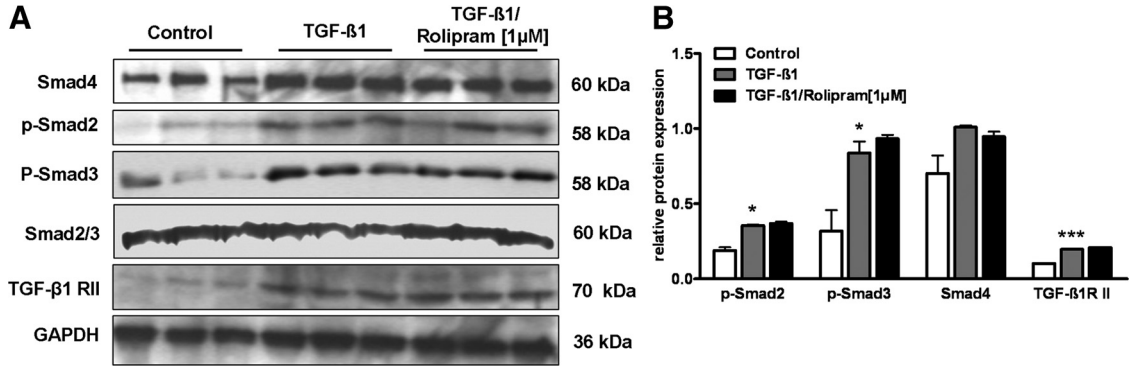

Figure 7. Effect of PDE4 inhibition on TGF-β1–induced Smad signaling. A549 cells were pretreated with PDE4 inhibitor rolipram (100 nM or 1 μM) for 12 h followed by TGF-β1 (2 ng/ml) stimulation for 24 h or stimulated with TGF-β1 (2 ng/ml) alone. (A) Protein expression as analyzed by immunoblotting. (B) Subsequent densitometric quantification of phospho-Smad2 (p-Smad2), phospho-Smad3 (p-Smad3) to Smad2/3, Smad4 and TGF-β1 RII in the above-mentioned treated cells. All values are given as the mean ± SEM (n = 4) and are normalized to GAPDH. *$p < 0.05$, **$p < 0.01$, and ***$p < 0.001$ versus control.

protein level (PDE10C, G, and H). However, it did not result in spontaneous mesenchymal marker induction (PDE10E–H). This indicates that PDE4 is important for the loss of epithelial phenotype but not sufficient for the induction of EMT in these cells.

DISCUSSION

This study has six salient findings. First, phosphodiesterases isoforms are significantly altered in TGF-β1–induced EMT. Second, cAMP-PDE activity and cAMP-PDEs PDE4A and PDE4D are significantly increased in TGF-β1–induced EMT. Third, inhibition of PDE4 by rolipram or PDE4 siRNA attenuated the genes associated with EMT. Fourth, PDE4 inhibition mediates EMT progression in a Smad-independent manner by inhibiting ROS production and p38 and ERK activation. Fifth, overexpression of PDE4A and/or PDE4D is important for the loss of epithelial phenotype but not sufficient for the induction of EMT in these cells. Sixth, inhibition of ROCK by Y-27632 or Rho siRNA suggests that Rho kinase signaling activated by TGF-β1 during EMT is a positive regulator of PDE4. This study supports a central role for PDE4 in the mechanism of EMT, and to our knowledge it is the first report demonstrating attenuation of epithelial mesenchymal transition by PDE4 inhibition.

The epithelial mesenchymal transition has emerged as a critical event not only in development but also in wound healing, fibrosis, and the invasion and metastasis of tumor cells (Greenburg and Hay, 1982; Thiery, 2002; Nawshad *et al*., 2005). Moreover, it has been recently established that EMT is critically involved in organ fibrosis, including the lung. It is increasingly being recognized that, after epithelial injury, epithelial cells can give rise to fibroblasts and thereby contribute to the pathogenesis of pulmonary fibrosis by undergoing EMT (Willis *et al*., 2005; Kim *et al*., 2006). Similarly, EMT involvement in lung cancer has been recently reported to promote the migratory and invasive abilities of lung cancer cells, attributes essential for tumor metastasis (Keshamouni *et al*., 2006).

We used TGF-β1 to induce EMT in A549 cells, because TGF-β1 has been shown to be a major regulator of EMT and A549 cells are among the best-characterized alveolar epithelial cells and have been used in several studies to investigate various aspects of EMT (Kasai *et al*., 2005; Illman *et al*., 2006; Keshamouni *et al*., 2006). Exposure of A549 cells to TGF-β1 for 24 h induced a complete conversion of the epithelial cells to myofibroblasts, as evidenced by the acquisition of a spindle-like morphology, the loss of epithelial marker genes (E-cadherin, zona occludens-1, and cytokeratin-18) and the gain of mesenchymal marker genes (fibronectin, desmin, and α-smooth muscle actin). The time frame required for this transition was similar to previous reports (Kasai *et al*., 2005). Exploring the involvement of PDEs in this established EMT model, we found the most striking twofold increase in total cAMP-PDE activity. Furthermore, real-time RT-PCR, immunoblotting, and immunofluorescence indicated that changes in the relative expression of PDE isoforms is accompanied TGF-β1–induced EMT, with an increased contribution of PDE4A and PDE4D, and a decreased role of PDE1 and PDE3 relative to control A549 cells. mRNA expression of PDE4A and PDE4D was increased by TGF-β1 as early as 6 h after stimulation (Figure 2C) and protein expression after 24 h. Interestingly, experiments with CHX indicate that TGF-β1 has no influence on posttranslationally PDE4 enzymatic activity. However, decreased expression of PDE1 and PDE3 isoforms can be markers of phenotypic switch. A reduction in PDE3/PDE4 activity as well as marked reductions in PDE3A mRNA and protein levels was observed during vascular smooth muscle cell phenotypic switch (Dunkerley *et al*., 2002). Similarly, inhibition of cytoplasmic PDE1A inhibited contractile phenotype in vascular smooth muscle cells (Nagel *et al*., 2006). Although not studied in detail in epithelial transition processes, we presume that down-regulation of PDE1 and PDE3 may have a functional relevance in these processes.

Most importantly, the PDE4 inhibitor rolipram exhibited a remarkable inhibitory effect on TGF-β1–induced EMT. This inhibition was complete, as evidenced by a restoration of epithelial morphology and E-cadherin expression and a complete abolishment of fibronectin stimulation. Interestingly, these effects were observed with a PDE4 inhibitor at very low concentrations (0.1–1 μM). These observations strongly suggest that potent inhibition of TGF-β1 induced the EMT by the PDE4 inhibitors. In agreement, specific inhibition of PDE4 isoforms by transfections with either PDE4A siRNA or PDE4D siRNA alone abolished TGF-β1–stimulated E-cadherin repression and fibronectin induction. However, combined together both siRNA showed no additive effects on these markers compared with individual siRNA. In general agreement with this observation, Zhang *et al*. (2006) demonstrated that the cAMP-elevating agents 8-bromo-cAMP and forskolin exhibit an inhibitory effect on

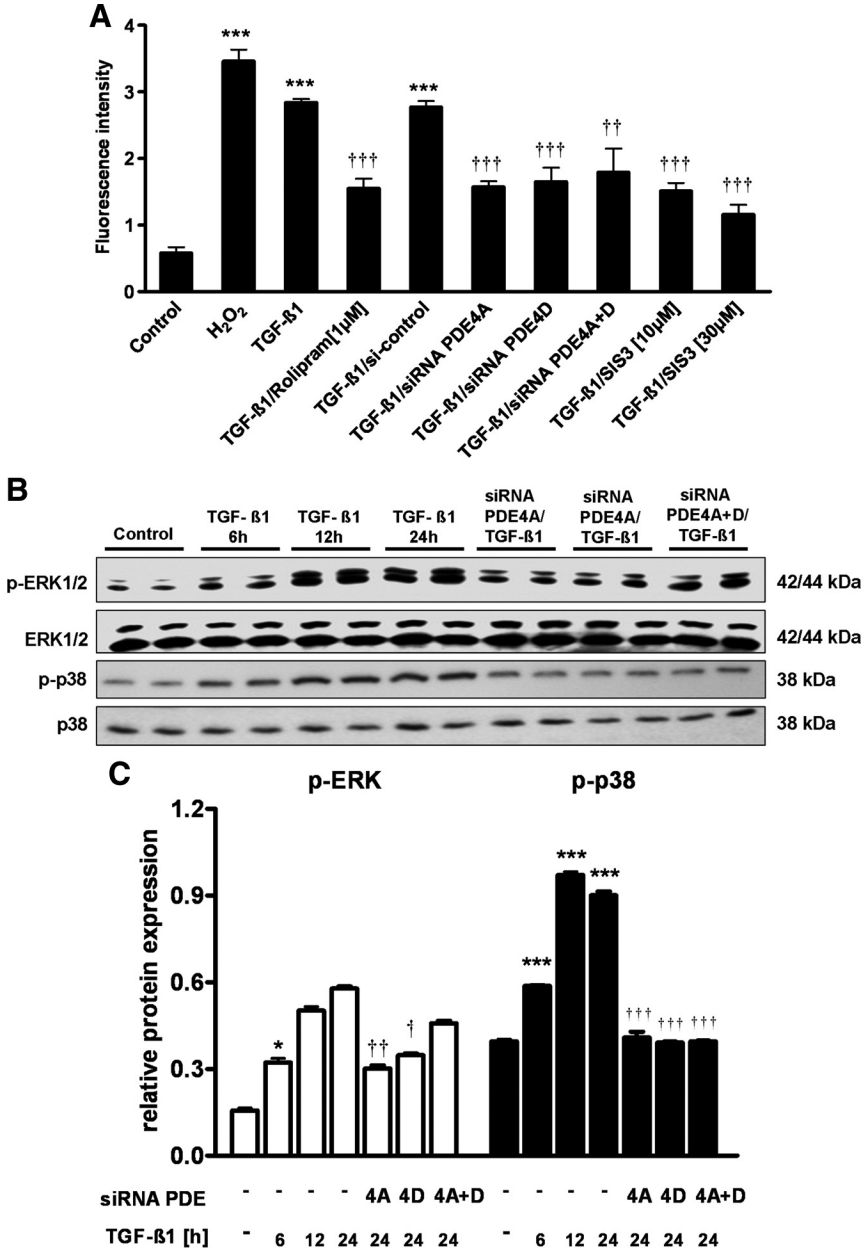

Figure 8. Effect of PDE4 knockdown and inhibition on ROS production, ERK, and p38 phosphorylation. A549 cells were treated with TGF-β1 (2 ng/ml) alone; pretreated with PDE4 inhibitor rolipram (1 μM) for 12 h followed by TGF-β1 (2 ng/ml) stimulation for 24 h; and transiently transfected with 100 nM PDE4A siRNA, PDE4D siRNA, or both (PDE4A+PDE4D) siRNAs for 48 h followed by TGF-β1 (2 ng/ml) stimulation for 24 h or treated with H_2O_2 (10 mM) for 12 h. (A) ROS production was measured by DHE fluorescence in 10 randomly selected images from each group. H_2O_2 served as a positive control. *$p < 0.05$, **$p < 0.01$, and ***$p < 0.001$ versus control; †$p < 0.05$, ††$p < 0.01$, and †††$p < 0.001$ versus TGF-β1–stimulated cells. (B) Protein expression of p-ERK, ERK, p-p38, and p38 as analyzed by immunoblotting. (C) Subsequent densitometric quantification of p-ERK to ERK and p-p38 to p38. All values are given as the mean ± SEM (n = 4) and are normalized to total ERK, p38 abundance. *$p < 0.05$, **$p < 0.01$, and ***$p < 0.001$ versus control; †$p < 0.05$, ††$p < 0.01$, and †††$p < 0.001$ versus TGF-β1–stimulated cells.

EMT in kidney epithelial cells. In contrast, the ectopic overexpression of PDE4A and/or PDE4D resulted in a significant loss of epithelial marker E-cadherin but did not result in changes of mesenchymal markers, indicating that PDE4 is important for the loss of epithelial phenotype but not sufficient enough for the induction of EMT in these cells.

TGF-β1 is known to exert its effects by binding to the TGF-β type II receptor (TβRII) and subsequently recruiting the TβRI. Smad2/3 and Smad4 are known intracellular mediators of TGF-β1. Once phosphorylated by the activated TGF-β1 receptor, Smad2 and/or Smad3 complex with Smad4 and translocate to the nucleus where they regulate TGF-β1 target genes (Nakao *et al*., 1997; Massague, 2000; Zavadil and Bottinger, 2005). In contrast, TGF-β1 can also regulate its target genes via non–Smad-dependent pathways that include the RhoA, Ras, MAPK, phosphatidylinositol 3-kinase, Notch, and Wnt signaling pathways (Bakin *et al*., 2000; Bhowmick *et al*., 2001; Moustakas and Heldin, 2005). The intracellular signaling pathways involved in PDE4 inhibition attenuated TGF-β1–mediated alveolar EMT; we found that TGF-β1 induces Smad2 and Smad3 phosphorylation in A549 cells, as has been shown by several other groups (Kasai *et al*., 2005). Interestingly, these phosphorylation events are not altered by PDE4 inhibition, suggesting that PDE4 inhibitors may use alternative Smad-independent pathways to regulate EMT marker genes.

Furthermore, considering the established role of PDE4 in inflammation and ROS generation (Jacob *et al*., 2002, 2004; Foucaud *et al*., 2007), we postulated ROS signaling to be a candidate mediator of the above-mentioned PDE4 inhibitory effects on EMT. Consistent with our hypothesis, we found that TGF-β1 induced a threefold increase in dichlorofluorescein-sensitive cellular ROS, confirming the report by Rhyu *et al*. (2005) in tubular epithelial cells (Rhyu *et al*., 2005). To our surprise, 1 μM PDE4 inhibitor PDE4 siRNA or Smad3 inhibitor completely blocked TGF-β1–induced ROS produc-

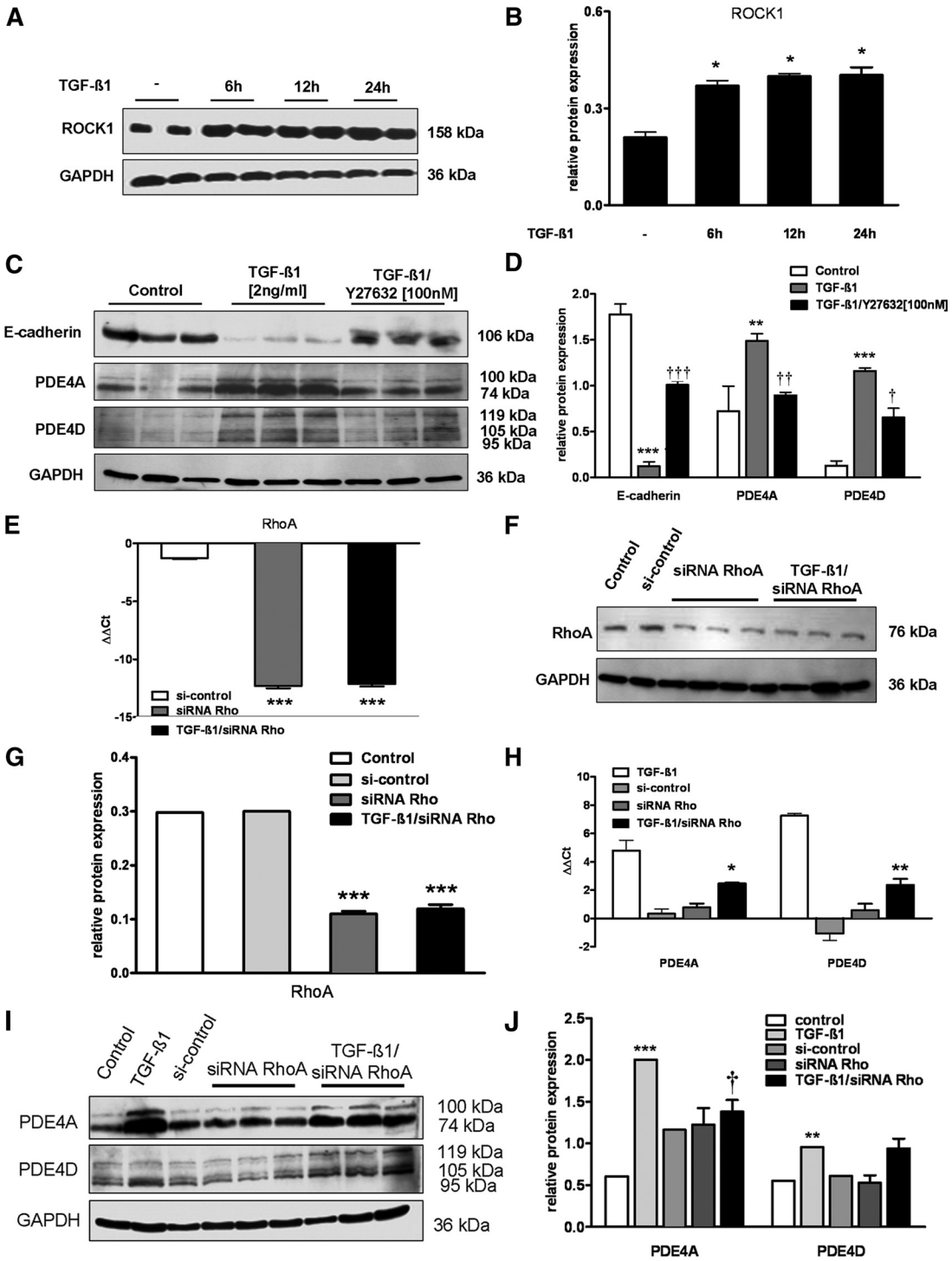

Figure 9. Effect of ROCK inhibition and RhoA knockdown on TGF-β1–induced EMT. (A) Protein expression. (B) Subsequent densitometric quantification of ROCK1 in A549 cells after TGF-β1 (2 ng/ml) stimulation for 6, 12, and 24 h. (C) Protein expression as analyzed by immunoblotting. (D) Subsequent densitometric quantification of E-cadherin, PDE4A, and PDE4D in A549 cells pretreated with the ROCK1 inhibitor Y-27632 (100 nM) for 12 h followed by TGF-β1 (2 ng/ml) stimulation for 24 h or stimulated with TGF-β1 (2 ng/ml) alone. (E and H) mRNA expression as analyzed by real-time RT-PCR. (F and I) Protein expression as analyzed by immunoblotting. (G and J) Subsequent densitometric quantification of RhoA, PDE4A, and PDE4D, respectively, in A549 cells transiently transfected with 100 nM control siRNA (si-control) or 100 nM RhoA siRNA for 24 h (mRNA expression) or 48 h (protein expression) followed by TGF-β1 (2 ng/ml) stimulation. All values are given as the mean ± SEM (n = 4) and are normalized to PBGD (E and H) or GAPDH (B, D, G, and J). *$p < 0.05$, **$p < 0.01$, and ***$p < 0.001$; †$p < 0.05$, ††$p < 0.01$, and †††$p < 0.001$ versus TGF-β1–stimulated cells.

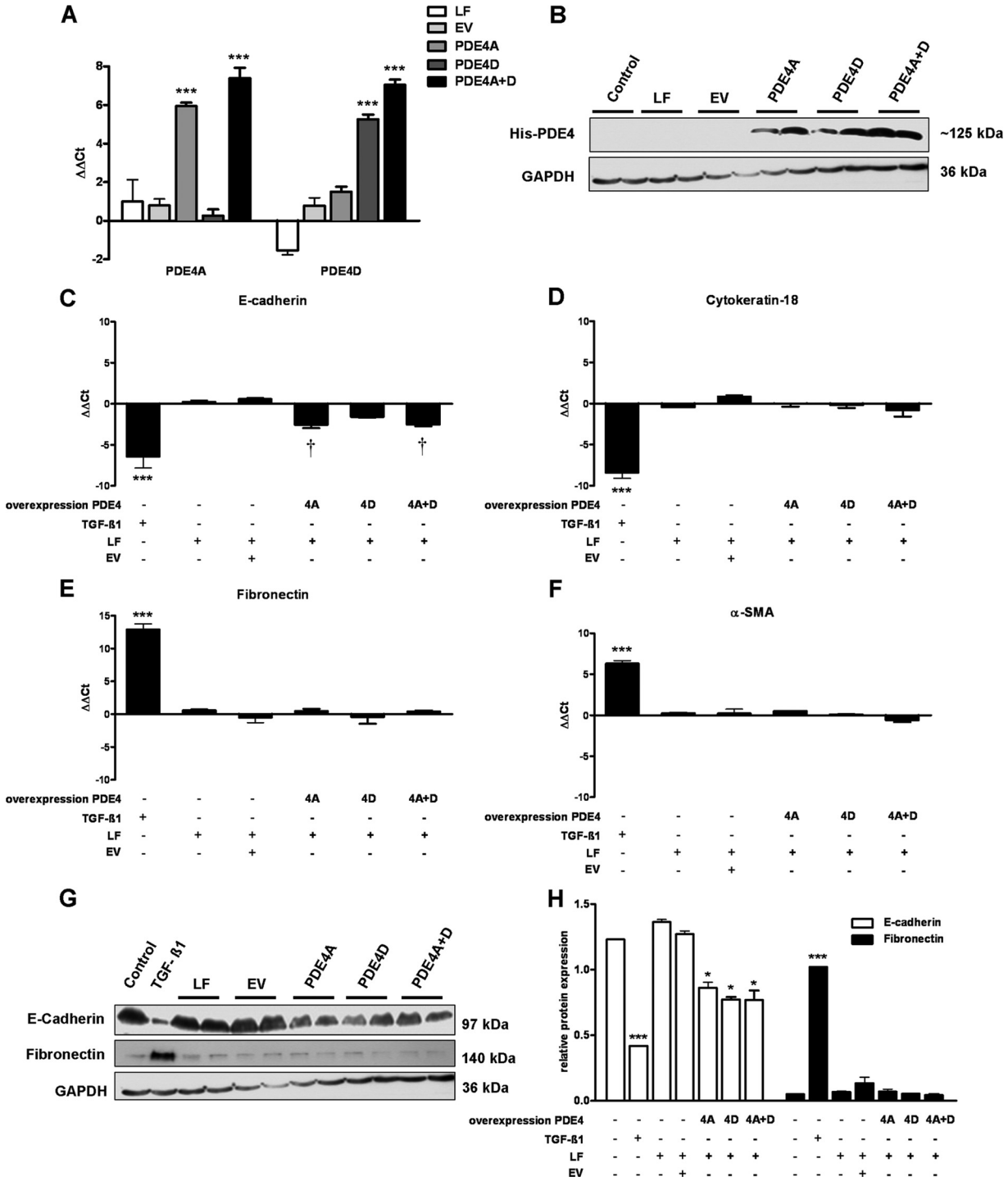

Figure 10. Effects of PDE4 overexpression in inducing epithelial mesenchymal transition. A549 cells were treated with TGF-β1 (2 ng/ml) for 24 h or transiently transfected with 2 μg empty vector (EV), PDE4A clone, PDE4D clone, or both (PDE4A+PDE4D). Lipofectamine (LF) was used as a transfection reagent. (A) mRNA expression of PDE4A and PDE4D as analyzed by real-time RT-PCR. (B) Protein expression of His tag as analyzed by immunoblotting in transfected cells. mRNA expression of E-cadherin (C), cytokeratin-18 (D), fibronectin (E), and α-SMA (F) as analyzed by real-time RT-PCR. (G) Protein expression as analyzed by immunoblotting. (H) Subsequent densitometric quantification of E-cadherin and fibronectin in above-mentioned transfected cells. *$p < 0.05$, **$p < 0.01$, and ***$p < 0.001$; †$p < 0.05$, ††$p < 0.01$, and †††$p < 0.001$ versus EV-transfected cells.

tion, thus establishing ROS as a target of PDE4 and Smad3 during EMT. This study also suggests that ROS may be downstream of Smad signaling. On the contrary, Rhyu *et al*. (2005) demonstrated that ROS are required for Smad phosphorylation downstream from TGF-β1. This apparent discrepancy in both studies can be due to several reasons: different concentration of TGF-β (2 vs. 10 ng/ml), different mode of action of the inhibitors: rolipram may inhibit ROS

generation in a Smad-independent manner via regulating other signaling pathways such as ERK-1/2 and p38 (Cheng *et al*., 2005) compared with antioxidants. In agreement with these observations, our data also suggest that rolipram inhibits phosphorylation of both p38 and ERK. Furthermore, studies from Black *et al*. (2007) suggest that Smad3 (+/+) hepatocytes treated with TGF-β1 displayed ROS generation compared with Smad3 (−/−) hepatocytes, suggesting a cross regulation of both Smad and ROS signaling.

Because recent studies have implicated the small GTPase Rho and its downstream effector Rho kinase (ROCK) in TGF-β1–induced remodeling of cell contacts in mammary epithelial cells, and as necessary components for the acquisition of stress fibers and a fibroblastic morphology in NMuMG and primary mouse keratinocytes (Bhowmick *et al*., 2001), we examined the possibility that PDE4 may influence EMT via Rho signaling. We found that TGF-β1–induced E-cadherin down-regulation is potently suppressed by the Rho kinase inhibitor Y-27632. Interestingly, to our surprise, Y-27632 as well as RhoA siRNA also decreased PDE4A and PDE4D expression, and subsequently PDE4 activity. Hence, to our knowledge, this is the first report suggesting a Rho/ROCK kinase signaling-dependent positive regulation of PDE4 or PDE4 induction.

In conclusion, the current study provides new evidence for a biochemical and physiologically important role for PDE isoforms in the epithelial mesenchymal transition in alveolar epithelial cells. Based on its high level of expression and activity, PDE4 seems to be a particularly useful marker of the phenotypic switch mediated by TGF-β1. The use of specific inhibitors targeted to cAMP hydrolyzing PDEs whose expression is increased during TGF-β1–induced EMT has the potential to provide a means to regulate the magnitude and duration of cAMP levels and response, and thereby to attenuate EMT. PDE4-selective inhibitors seem to be particularly attractive as novel therapeutics to attenuate EMT-associated lung diseases, such as pulmonary fibrosis and lung cancer.

ACKNOWLEDGMENTS

Ewa Kolosionek received a predoctoral fellowship from Nycomed (Konstanz, Germany). This work was supported by the "Deutsche Forschungsgemeinschaft" KFO 118, projects TP 3 and TP 7; the European Commission under the Sixth Frame work Programme (LSHM-CT-2005-018725, PULMOTENSION); and the STARTUP AWARD from Justus-Liebig University (Giessen, Germany).

REFERENCES

Bakin, A. V., Tomlinson, A. K., Bhowmick, N. A., Moses, H. L., and Arteaga, C. L. (2000). Phosphatidylinositol 3-kinase function is required for transforming growth factor beta-mediated epithelial to mesenchymal transition and cell migration. J. Biol. Chem. *275*, 36803–36810.

Bender, A. T., Ostenson, C. L., Wang, E. H., and Beavo, J. A. (2005). Selective up-regulation of PDE1B2 upon monocyte-to-macrophage differentiation. Proc. Natl. Acad. Sci. USA *102*, 497–502.

Bhowmick, N. A., Ghiassi, M., Bakin, A., Aakre, M., Lundquist, C. A., Engel, M. E., Arteaga, C. L., and Moses, H. L. (2001). Transforming growth factor-beta1 mediates epithelial to mesenchymal transdifferentiation through a RhoA-dependent mechanism. Mol. Biol. Cell *12*, 27–36.

Black, D., Lyman, S., Qian, T., Lemasters, J. J., Rippe, R. A., Nitta, T., Kim, J. S., and Behrns, K. E. (2007). Transforming growth factor beta mediates hepatocyte apoptosis through Smad3 generation of reactive oxygen species. Biochimie *89*, 1464–1473.

Brown, K. A., Pietenpol, J. A., and Moses, H. L. (2007). A tale of two proteins: differential roles and regulation of Smad2 and Smad3 in TGF-beta signaling. J. Cell. Biochem. *101*, 9–33.

Cheng, J., Diaz Encarnacion, M. M., Warner, G. M., Gray, C. E., Nath, K. A., and Grande, J. P. (2005). TGF-beta1 stimulates monocyte chemoattractant protein-1 expression in mesangial cells through a phosphodiesterase isoenzyme 4-dependent process. Am. J. Physiol. Cell Physiol. *289*, C959–C970.

Conti, M., and Beavo, J. (2007). Biochemistry and physiology of cyclic nucleotide phosphodiesterases: essential components in cyclic nucleotide signaling. Annu. Rev. Biochem. *76*, 481–511.

Dunkerley, H. A., Tilley, D. G., Palmer, D., Liu, H., Jimmo, S. L., and Maurice, D. H. (2002). Reduced phosphodiesterase 3 activity and phosphodiesterase 3A level in synthetic vascular smooth muscle cells: implications for use of phosphodiesterase 3 inhibitors in cardiovascular tissues. Mol. Pharmacol. *61*, 1033–1040.

Dunkern, T. R., Feurstein, D., Rossi, G. A., Sabatini, F., and Hatzelmann, A. (2007). Inhibition of TGF-beta induced lung fibroblast to myofibroblast conversion by phosphodiesterase inhibiting drugs and activators of soluble guanylyl cyclase. Eur. J. Pharmacol. *572*, 12–22.

Foucaud, L., Wilson, M. R., Brown, D. M., and Stone, V. (2007). Measurement of reactive species production by nanoparticles prepared in biologically relevant media. Toxicol. Lett. *174*, 1–9.

Ghofrani, H. A., Wiedemann, R., Rose, F., Schermuly, R. T., Olschewski, H., Weissmann, N., Gunther, A., Walmrath, D., Seeger, W., and Grimminger, F. (2002). Sildenafil for treatment of lung fibrosis and pulmonary hypertension: a randomised controlled trial. Lancet *360*, 895–900.

Greenburg, G., and Hay, E. D. (1982). Epithelia suspended in collagen gels can lose polarity and express characteristics of migrating mesenchymal cells. J. Cell Biol. *95*, 333–339.

Higgins, D. F., *et al*. (2007). Hypoxia promotes fibrogenesis in vivo via HIF-1 stimulation of epithelial-to-mesenchymal transition. J. Clin. Invest. *117*, 3810–3820.

Huang, Z., and Mancini, J. A. (2006). Phosphodiesterase 4 inhibitors for the treatment of asthma and COPD. Curr. Med. Chem. *13*, 3253–3262.

Illman, S. A., Lehti, K., Keski-Oja, J., and Lohi, J. (2006). Epilysin (MMP-28) induces TGF-beta mediated epithelial to mesenchymal transition in lung carcinoma cells. J. Cell Sci. *119*, 3856–3865.

Jacob, C., Martin-Chouly, C., and Lagente, V. (2002). Type 4 phosphodiesterase-dependent pathways: role in inflammatory processes. Therapie *57*, 163–168.

Jacob, C., Szilagyi, C., Allen, J. M., Bertrand, C., and Lagente, V. (2004). Role of PDE4 in superoxide anion generation through p44/42MAPK regulation: a cAMP and a PKA-independent mechanism. Br. J. Pharmacol. *143*, 257–268.

Jiang, Z., Seo, J. Y., Ha, H., Lee, E. A., Kim, Y. S., Han, D. C., Uh, S. T., Park, C. S., and Lee, H. B. (2003). Reactive oxygen species mediate TGF-beta1-induced plasminogen activator inhibitor-1 upregulation in mesangial cells. Biochem. Biophys. Res. Commun. *309*, 961–966.

Kalluri, R., and Neilson, E. G. (2003). Epithelial-mesenchymal transition and its implications for fibrosis. J. Clin. Invest. *112*, 1776–1784.

Kasai, H., Allen, J. T., Mason, R. M., Kamimura, T., and Zhang, Z. (2005). TGF-beta1 induces human alveolar epithelial to mesenchymal cell transition (EMT). Respir. Res. *6*, 56.

Keshamouni, V. G., *et al*. (2006). Differential protein expression profiling by iTRAQ-2DLC-MS/MS of lung cancer cells undergoing epithelial-mesenchymal transition reveals a migratory/invasive phenotype. J. Proteome Res. *5*, 1143–1154.

Kim, K. K., Kugler, M. C., Wolters, P. J., Robillard, L., Galvez, M. G., Brumwell, A. N., Sheppard, D., and Chapman, H. A. (2006). Alveolar epithelial cell mesenchymal transition develops in vivo during pulmonary fibrosis and is regulated by the extracellular matrix. Proc. Natl. Acad. Sci. USA *103*, 13180–13185.

Liu, X., Sun, S. Q., Hassid, A., and Ostrom, R. S. (2006). cAMP inhibits transforming growth factor-beta-stimulated collagen synthesis via inhibition of extracellular signal-regulated kinase 1/2 and Smad signaling in cardiac fibroblasts. Mol. Pharmacol. *70*, 1992–2003.

Massague, J. (2000). How cells read TGF-beta signals. Nat. Rev. Mol. Cell Biol. *1*, 169–178.

Miettinen, P. J., Ebner, R., Lopez, A. R., and Derynck, R. (1994). TGF-beta induced transdifferentiation of mammary epithelial cells to mesenchymal cells: involvement of type I receptors. J. Cell Biol. *127*, 2021–2036.

Moustakas, A., and Heldin, C. H. (2005). Non-Smad TGF-beta signals. J. Cell Sci. *118*, 3573–3584.

Moustakas, A., and Heldin, C. H. (2007). Signaling networks guiding epithelial-mesenchymal transitions during embryogenesis and cancer progression. Cancer Sci. *98*, 1512–1520.

Murray, F., Patel, H. H., Suda, R. Y., Zhang, S., Thistlethwaite, P. A., Yuan, J. X., and Insel, P. A. (2007). Expression and activity of cAMP phosphodies-

terase isoforms in pulmonary artery smooth muscle cells from patients with pulmonary hypertension: role for PDE1. Am. J. Physiol Lung Cell Mol. Physiol. *292*, L294–L303.

Nagel, D. J., *et al*. (2006). Role of nuclear Ca2+/calmodulin-stimulated phosphodiesterase 1A in vascular smooth muscle cell growth and survival. Circ. Res. *98*, 777–784.

Nakao, A., *et al*. (1997). TGF-beta receptor-mediated signalling through Smad2, Smad3 and Smad4. EMBO J. *16*, 5353–5362.

Naro, F., Sette, C., Vicini, E., De, A. V., Grange, M., Conti, M., Lagarde, M., Molinaro, M., Adamo, S., and Nemoz, G. (1999). Involvement of type 4 cAMP-phosphodiesterase in the myogenic differentiation of L6 cells. Mol. Biol. Cell *10*, 4355–4367.

Nawshad, A., Lagamba, D., Polad, A., and Hay, E. D. (2005). Transforming growth factor-beta signaling during epithelial-mesenchymal transformation: implications for embryogenesis and tumor metastasis. Cells Tissues. Organs *179*, 11–23.

Rees, J. R., Onwuegbusi, B. A., Save, V. E., Alderson, D., and Fitzgerald, R. C. (2006). In vivo and in vitro evidence for transforming growth factor-beta1-mediated epithelial to mesenchymal transition in esophageal adenocarcinoma. Cancer Res. *66*, 9583–9590.

Rhyu, D. Y., Yang, Y., Ha, H., Lee, G. T., Song, J. S., Uh, S. T., and Lee, H. B. (2005). Role of reactive oxygen species in TGF-beta1-induced mitogen-activated protein kinase activation and epithelial-mesenchymal transition in renal tubular epithelial cells. J. Am. Soc. Nephrol. *16*, 667–675.

Santibanez, J. F., Olivares, D., Guerrero, J., and Martinez, J. (2003). Cyclic AMP inhibits TGFbeta1-induced cell-scattering and invasiveness in murine-transformed keratinocytes. Int. J. Cancer *107*, 715–720.

Savai, R., Schermuly, R. T., Pullamsetti, S. S., Schneider, M., Greschus, S., Ghofrani, H. A., Traupe, H., Grimminger, F., and Banat, G. A. (2007). A combination hybrid-based vaccination/adoptive cellular therapy to prevent tumor growth by involvement of T cells. Cancer Res. *67*, 5443–5453.

Savai, R., Schermuly, R. T., Voswinckel, R., Renigunta, A., Reichmann, B., Eul, B., Grimminger, F., Seeger, W., Rose, F., and Hanze, J. (2005). HIF-1alpha attenuates tumor growth in spite of augmented vascularization in an A549 adenocarcinoma mouse model. Int. J. Oncol. *27*, 393–400.

Schermuly, R. T., *et al*. (2007). Phosphodiesterase 1 upregulation in pulmonary arterial hypertension: target for reverse-remodeling therapy. Circulation *115*, 2331–2339.

Thiery, J. P. (2002). Epithelial-mesenchymal transitions in tumour progression. Nat. Rev. Cancer *2*, 442–454.

Thompson, W. J., and Appleman, M. M. (1971). Multiple cyclic nucleotide phosphodiesterase activities from rat brain. Biochemistry *10*, 311–316.

Vyas-Read, S., Shaul, P. W., Yuhanna, I. S., and Willis, B. C. (2007). Nitric oxide attenuates epithelial-mesenchymal transition in alveolar epithelial cells. Am. J. Physiol Lung Cell Mol. Physiol *293*, L212–L221.

Willis, B. C., and Borok, Z. (2007). TGF-beta-induced EMT: mechanisms and implications for fibrotic lung disease. Am. J. Physiol Lung Cell Mol. Physiol. *293*, L525–L534.

Willis, B. C., Liebler, J. M., Luby-Phelps, K., Nicholson, A. G., Crandall, E. D., du Bois, R. M., and Borok, Z. (2005). Induction of epithelial-mesenchymal transition in alveolar epithelial cells by transforming growth factor-beta *1*, potential role in idiopathic pulmonary fibrosis. Am. J. Pathol. *166*, 1321–1332.

Zavadil, J., and Bottinger, E. P. (2005). TGF-beta and epithelial-to-mesenchymal transitions. Oncogene *24*, 5764–5774.

Zhang, A., Dong, Z., and Yang, T. (2006). Prostaglandin D2 inhibits TGF-beta1-induced epithelial-to-mesenchymal transition in MDCK cells. Am. J. Physiol Renal Physiol *291*, F1332–F1342.